

Comparison of Two Fractional-Order High-Order SMC Techniques for DFIG-Based Wind Turbines: Theory and Simulation Results

Ali Nadhim Jbarah Almakki^{1,2†}, Andrey Mazalov³,
Habib Benbouhenni⁴, and Nicu Bizon^{5,6,7}, Non-members

ABSTRACT

Two new nonlinear techniques are proposed in this study for improving the performance and efficiency of the doubly-fed induction generator (DFIG)-based wind turbine systems. Direct torque control (DTC) is among the most widely used strategies for controlling DFIGs due to its many advantages, such as robustness, simplicity, and fast response dynamics. However, this control causes big ripples in both torque and flux. Furthermore, it has significant total harmonic distortion (THD). Several solutions are proposed to overcome these problems, including nonlinear techniques and intelligent strategies such as genetic algorithms. In this work, two different controllers are proposed to improve the performance of the DTC technique. Firstly, the second-order continuous sliding mode (SOCSM) based on fractional-order (FO) control, and secondly, the super twisting algorithm (STA) based on the FO technique. The biggest advantages of the proposed strategies are their durability and ease of execution. Based on the proposed controls, the DTC strategy can greatly improve generator performance in different operating conditions. This paper also provides a comparative analysis of DTC-FOSOCSCM, DTC, and DTC-FOSTA in terms of reference tracking, robustness, chattering reduction, and computational complexity, using mathematical theory and simulation carried out in Matlab/Simulink using a 1.5 MW DFIG-based wind turbine. The simulation results demonstrate the effectiveness and high performance of the proposed DTC techniques.

Keywords: Doubly-fed induction generators, Total harmonic distortion, Fractional calculus, Super twisting algorithms, Second-order continuous sliding mode, Wind turbine

1. INTRODUCTION

In recent years, electricity demand has increased significantly, and traditional sources alone are becoming insufficient. There are numerous and varied reasons for this rising demand, such as high temperatures and the widespread use of electric motors and electrical appliances. Technology has invaded our daily lives, with telephones and electronic media becoming necessities. Therefore, other sources of inexpensive and clean electricity generation must be found [1].

Several solutions have been proposed to compensate for the use of petroleum, including nuclear energy. However, despite the advantages and value of the electrical energy produced through this method, it remains harmful to human health and nature. In recent years, other sources not harmful to human health while also limiting the spread of toxic gases have been identified under the term renewable energy. It depends on the use of natural elements, such as wind and solar energy.

Wind energy is among the most widely used form of renewable energy in the world, with wind farms (wind stations) scattered around the world due to its low cost and ease of use compared to other sources [2]. To generate electricity from wind, electric generators powered by turbines are used. The latter converts wind energy into mechanical energy which is then used to rotate the generator. The rotation of the generator leads to the production of electrical energy.

¹The author is with College of Engineering, University of Diyala, Diyala, Iraq,

²The author is with Department of Electrical Equipment, Kazan National Research Technical University named after A. N. Tupolev – KAI, Kazan, Russia,

³The author is with Department of Electrical Engineering and Mechatronics, Southern Federal University, Rostov-On-Don, Russia,

⁴The author is with Unité de Recherche sur les Systèmes Intelligents Embarqués, Centre de Recherche sur l'Information Scientifique et Technique CERIST, Algiers, Algeria

⁵The author is with Doctoral School, Polytechnic University of Bucharest, 313 Splaiul Independentei, 060042 Bucharest, Romania

⁶The author is with Faculty of Electronics, Communication and Computers, University of Pitesti, 110040 Pitesti, Romania,

⁷The author is with ICSI Energy Department, National Research and Development Institute for Cryogenic and Isotopic Technologies, 240050 Ramnicu Valcea, Romania,

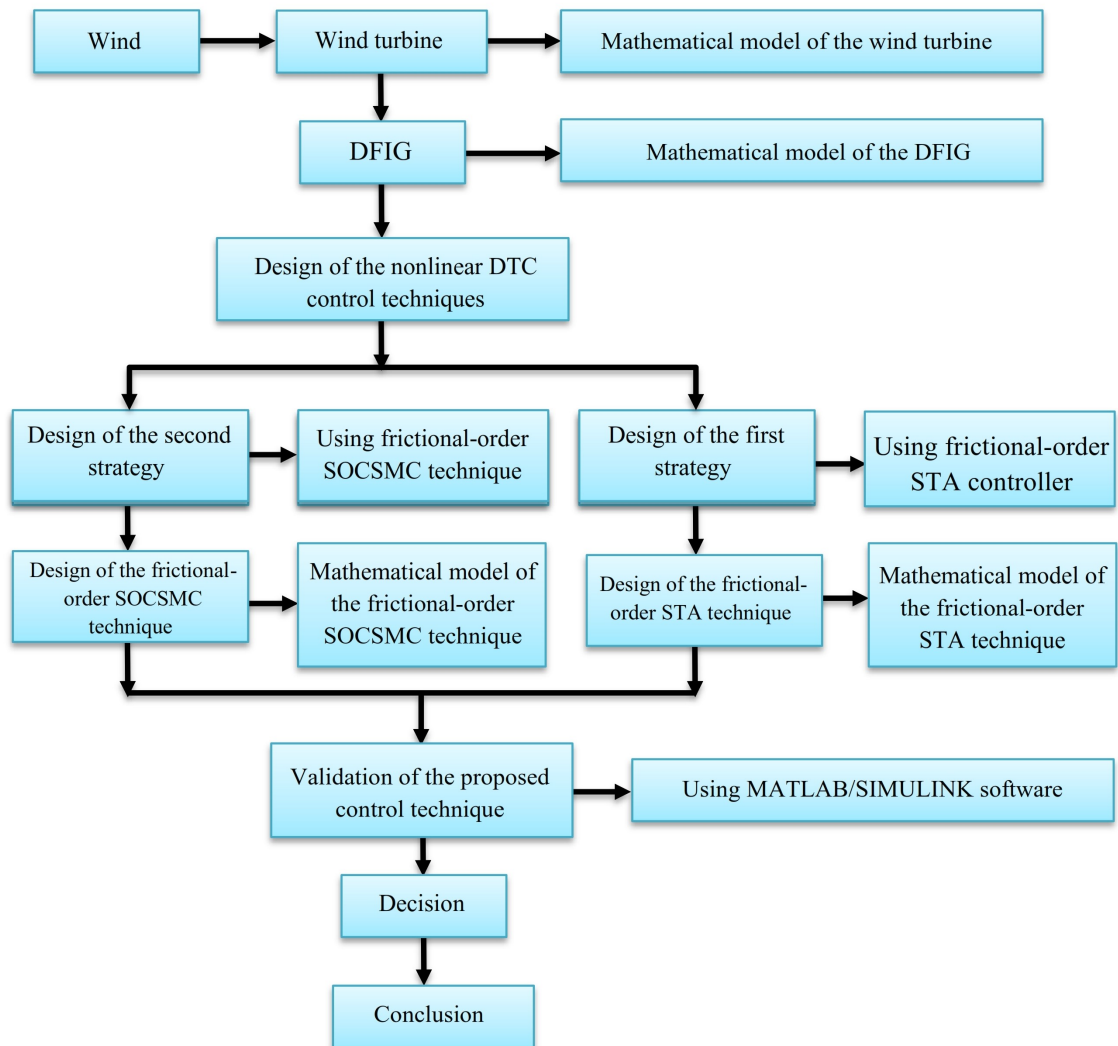
[†]Corresponding author: alinadhimj@gmail.com

©2023 Author(s). This work is licensed under a Creative Commons Attribution-NonCommercial-NoDerivs 4.0 License. To view a copy of this license visit: <https://creativecommons.org/licenses/by-nc-nd/4.0/>.

Digital Object Identifier: 10.37936/ecti-ec.2023212.249817

Table 1: A comparative study between the DTC and various published techniques.

| Criteria | Published Techniques | | | | | | |
|--------------------------------------|-----------------------|--------|-------------|-------------|-----------------------|-------------|--------------|
| | DARPC | DVC | IVC | SMC | DTC | SOSMC | Backstepping |
| Controller | Hysteresis Components | PI | PI | - | Hysteresis Components | - | - |
| Implementation | Easy | Easy | Difficult | Difficult | Easy | Difficult | Easy |
| Robustness | ++ | + | + | +++ | ++ | ++++ | ++++ |
| Response Dynamics | Good | Well | Good | Excellent | Good | Excellent | Excellent |
| Reference | +++ | + | ++ | +++ | +++ | ++++ | ++++ |
| Tracking | Simple | Simple | Complicated | Complicated | Simple | Complicated | Complicated |
| Improvement in transient performance | Good | Weak | Weak | Good | Good | Excellent | Excellent |

**Fig. 1:** Diagram for proposed nonlinear DTC control techniques.

Several generator types can be used in wind stations (farms), such as the squirrel cage asynchronous generator (SCAG), synchronous generator (SG), DC generator, doubly-fed induction generator (DFIG), etc. However, the DFIG remains the most widely used in this field due to its simplicity of control, robustness, and low cost. The DFIG also requires little maintenance and compares favorably to its counterparts in both characteristics and advantages [3]. Among the most widely used methods for controlling the DFIG are direct torque control (DTC) [4], synergetic control (SC) [5], backstepping control [6], sliding mode control (SMC) [7], direct power control (DPC) [8], field-oriented control (FOC) [9], and hybrid control [10–13].

Traditionally, the DTC technique is one of the most widely used strategies for controlling electric generators, such as the DFIG, induction motor (IM), and SGs, due to the characteristics and advantages it has over other methods. This control uses the same principle as the DPC technique, with a switching table and hysteresis comparators to control the torque and flux. In [9], the IM was controlled by the DTC technique. The results showed the effectiveness of this control in improving the performance and efficiency of the IM drive. In [14], DTC strategies were applied to control the dual open-end winding IM drive. On the other hand, the DTC control has previously been proposed to control both permanent magnet synchronous motors (PMSM) [15], brushless DC motor [16], SGs [17], DFIG [18], six-phase IM [19], five-phase IM [20], and six-phase synchronous motor [21].

A comparison can be made between this control and the various known strategies published in scientific papers such as FOC and DPC in terms of ease of implementation, robustness, and speed of response. Table 1 presents a comparative study between the DTC technique and the various strategies currently known to control electrical machines. In this control, the switching table is used to control the inverter rather than using the pulse width modulation (PWM) technique, as in the case of the FOC. The DTC technique is among the best and most robust and offers a very fast dynamic response compared to many other methods such as the FOC, direct vector control (DVC), and indirect vector control (IVC). However, this control has many drawbacks, including torque ripples, rotor flux ripples, and harmonic distortion of the stator current. Several recently published scientific works have suggested solutions for improving the performance of the DTC technique, such as the use of fuzzy logic, neural networks, a genetic algorithm, neuro-fuzzy algorithm, super twisting algorithm (STA), fractional-order control (FOC), second-order continuous sliding mode control (SOCSCMC), etc. Table 2 presents most of the works carried out to improve the performance and effectiveness of the DTC technique using nonlinear controllers and artificial intelligence. The controller used for improvement is mentioned in the table along with the results and type of study, whether experimental or simulated [3].

Several techniques have been used to improve the efficiency and properties of the traditional DTC strategy. However, their effectiveness differs from one controller to another. Researchers who relied on the use of nonlinear techniques only, and some combined nonlinear techniques with artificial intelligence to obtain a more robust control were able to improve the DTC technique [30].

This work proposes two nonlinear DTC techniques to control the DFIG-based wind power generation system. Two new nonlinear controllers are proposed to improve the performance and characteristics of the DTC strategy in the DFIG-based wind turbine. The two proposed nonlinear controllers consist of the fractional-order STA (FOSTA) controller and the fractional-order SOCSCMC (FOSOCSCMC) controller. These two new nonlinear controllers are proposed to minimize torque and flux ripples, as well as reducing the THD value of the stator current.

Two different DTC strategies are proposed to control the DFIG-based wind turbine, the first of which is the DTC-FOSTA technique and the second the DTC-FOSOCSCMC. The results obtained from these proposed DTC techniques were compared with those of the classical DTC strategy, in terms of electric current quality, ratio of torque and flux ripples, and degree of durability. The work carried out in this study is illustrated in Fig. 1. A diagram of the proposed nonlinear DTC techniques is also shown in Fig. 1, with two different conceptual approaches proposed for generator control. The obtained results were compared with the classical method.

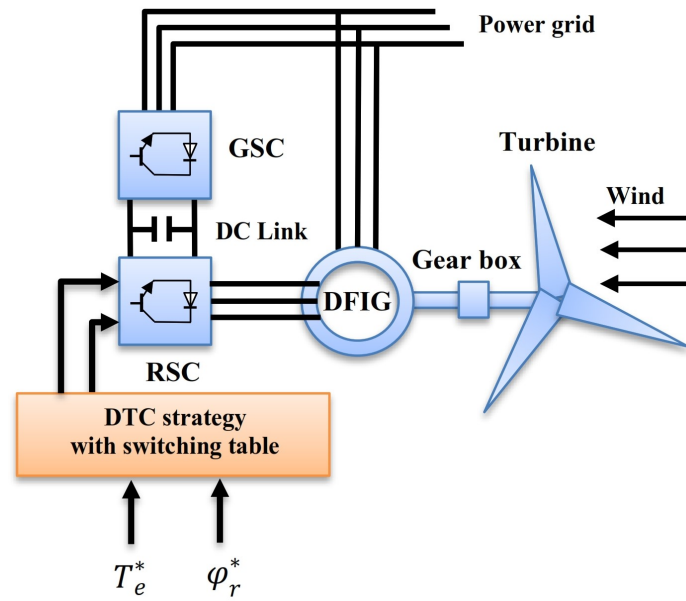
Consequently, the novelty and main contributions of this paper are as follows:

- A two nonlinear controller is designed and applied in the DTC strategy of the DFIG.
- Two nonlinear DTC strategies of the DFIG-based wind power system are proposed since they have more favorable characteristics than the DTC strategy while retaining the merits of its ease of execution and simplicity.
- The ripples of the flux and torque are reduced, and the inverter switching frequency mastered to limit the different problems of DFIG-based wind power systems.
- The proposed FOSTA and FOSOCSCMC controllers are used to reduce the THD value of the stator current.
- The characteristics of the DFIG controlled by the two proposed nonlinear DTC strategies are compared to those of the DFIG controlled by the DTC strategy to demonstrate performance improvement.

The comparative results confirm the good performance of the two proposed nonlinear DTC techniques, where the rotor flux, current and electromagnetic ripples, and the THD of the generated currents were significantly minimized, especially under a change in system parameters. Moreover, the simulation results indicate that the DTC-FOSTA technique is better in terms of ripple ratio and the THD current value than the DTC-FOSOCSCMC technique.

Table 2: Different methods for improving the DTC technique.

| References | Study Type | Electric Machine Type | The Type of Method Used | Torque Ripple | Flux Ripple | Ratio of THD | Robustness | Simplicity |
|------------|--------------|-----------------------|-----------------------------------------------|---------------|-------------|--------------|------------|-------------|
| [22] | Simulation | DFIG | Third-order SMC technique | Low | Low | Low | High | Simple |
| [23] | Simulation | Induction Motor | Three-level inverter | Medium | Medium | Medium | Low | Simple |
| [24] | Experimental | PMSM | Space vector modulation | Medium | Medium | Medium | Low | Simple |
| [25] | Simulation | PMSM | Sliding mode control | Medium | Medium | Medium | Medium | Complicated |
| [26] | Experimental | PMSM | Modified finite set model predictive strategy | Medium | Medium | Medium | Medium | Complicated |
| [27] | Simulation | DFIG | Fuzzy logic | Medium | Medium | Medium | Medium | Complicated |
| [28] | Simulation | Multi-phase PMSM | Feedforward neural network | Medium | Medium | Medium | Medium | Simple |
| [29] | Simulation | Multi-phase IPMSM | Fuzzy logic and SVM technique | Medium | Medium | Medium | High | Complicated |
| [30] | Simulation | DFIG | ANFIS-STA and SVM | Medium | Medium | Low | High | Complicated |
| [31] | Simulation | DFIG | Neural PI and modified SVM | Medium | Medium | Low | High | Simple |
| [32] | Simulation | DFIG | Second-order continuous sliding mode control | Medium | Medium | Low | High | Simple |

**Fig. 2:** Block diagram of a wind power system with a DFIG controlled by the DTC technique [33].

2. WIND POWER SYSTEM

Fig. 2 shows the electric power generation system using wind energy. This system requires a turbine to convert wind energy into mechanical energy to rotate the DFIG. A generator is also needed to convert mechanical energy into electrical energy. This system uses two inverters; one to convert AC to DC, and another for converting from DC to AC [33]. The system is very simple and easy to implement and can be easily controlled.

2.1 Model of the Wind Turbine

The mechanical energy obtained by the turbine is represented by Eq. (1). This energy is related to each of the wind speeds (v), tip speed ratio (λ), air density (ρ), radius of the turbine (R), blade pitch angle (β), and power coefficient (C_p) [34].

$$P_t = \frac{1}{2} R^2 \cdot V^3 C_p(\beta, \lambda) \quad (1)$$

Eq. (2) represents the power coefficient of the wind turbine.

$$C_p(\lambda, \beta) = (\beta - 2)(0.5 - 0.167) \sin\left(\frac{\pi(\lambda + 0.1)}{18.5 - 0.3(\beta - 2)}\right) - 0.0018 \times (\beta - 2)(\lambda - 3) \quad (2)$$

The tip speed ratio is represented by Eq. (3).

$$\lambda = \frac{\Omega_r \cdot R}{V} \quad (3)$$

where Ω_r is the rotational speed of the wind turbine.

2.2 The Mathematic Model of the DFIG

To study this system, the mathematical form of the turbine and DFIG must be given. Eqs. (4)-(8) represent the mathematical model of the DFIG used in this work [35, 36].

$$\begin{cases} V_{dr} = R_r I_{dr} - w_r \Psi_{qr} + \frac{d}{dt} \Psi_{dr} \\ V_{qr} = R_r I_{qr} + w_r \Psi_{dr} + \frac{d}{dt} \Psi_{qr} \\ V_{qs} = R_s I_{qs} + w_s \Psi_{ds} + \frac{d}{dt} \Psi_{qs} \\ V_{ds} = R_s I_{ds} - w_s \Psi_{qs} + \frac{d}{dt} \Psi_{ds} \end{cases} \quad (4)$$

The following equation interconnects the rotor and stator pulsations and rotor speed: $w_s = w_r + w$. Where w_r and w_s are the rotor and stator electrical pulsations, respectively, while w is the mechanical one.

The rotor and stator flux can be written as follows:

$$\begin{cases} \Psi_{dr} = M I_{ds} + L_r I_{dr} \\ \Psi_{qr} = M I_{qs} + L_r I_{qr} \\ \Psi_{ds} = M I_{dr} + L_s I_{ds} \\ \Psi_{qs} = M I_{qr} + L_s I_{qs} \end{cases} \quad (5)$$

$(V_{dr}, V_{qr}, V_{ds}, V_{qs})$, $(\Psi_{dr}, \Psi_{ds}, \Psi_{qs}, \Psi_{ds})$, $(I_{dr}, I_{qr}, I_{ds}, I_{qs})$, are the stator and rotor voltages, fluxes, and currents,

respectively; R_r and R_s are the resistances of the stator and rotor windings, respectively, while L_r , L_s , and M are the inductance rotor, stator, and mutual inductance between two coils, respectively.

The mechanical equation of the DFIG is given as:

$$T_e = T_r + J \cdot \frac{d\Omega}{dt} + F_r \cdot \Omega \quad (6)$$

The electromagnetic torque established by the DFIG can be written in terms of flux and current by Equation (7):

$$T_e = \frac{3}{2} \frac{M}{L_s} n_p (-\Psi_{ds} I_{qr} + \Psi_{qs} I_{dr}) \quad (7)$$

where J is the inertia, Ω is the mechanical rotor speed, T_r is the load torque, and F_r is the viscous friction coefficient.

The reactive and active powers of the stator side are defined as:

$$\begin{cases} Q_s = 1.5(-V_{ds} I_{qs} + V_{qs} I_{ds}) \\ P_s = 1.5(V_{qs} I_{qs} + V_{ds} I_{ds}) \end{cases} \quad (8)$$

3. TRADITIONAL DTC TECHNIQUE

The DTC strategy aims to regulate the torque and rotor flux using a switching table and two hysteresis comparators. The DTC technique is more efficient, simple, and robust than the FOC technique. The DTC strategy is more effective at improving the performance of electric machines than the FOC technique.

The DTC strategy has become one the most popular linear methods in recent years and used in the field of renewable energy, especially wind, because of its many advantages. Fig. 3 presents the traditional DTC technique of the DFIG using proportional-integral (PI) controllers. The inverter of the DFIG is controlled by the space vector modulation (SVM) strategy. This control scheme is simpler and easier to implement than the vector control and FOC strategies. Using the SVM technique to control the inverter increases system durability and helps improve the quality of the current. Compared to the pulse width modulation (PWM) technique, the SVM is better for obtaining a signal at the inverter output with a constant frequency. The SVM strategy is detailed in [37].

Among the disadvantages of this system are the estimation of both torque and rotor flux and, consequently, there is an urgent need for high-quality tension and current measuring devices.

The DTC technique based on traditional PI controllers represents a modification of the traditional DTC technique with a switching table. The PI controllers are used to regulate the quadrature and direct rotor voltages, as detailed in [22]. The DTC-PI technique is more robust than the FOC, DTC, and vector control strategies. In addition, the DTC-PI technique is better at reducing the torque and flux ripples than the FOC, vector control, and DTC strategies. Both the torque and rotor flux need to be estimated in this control scheme. Furthermore,

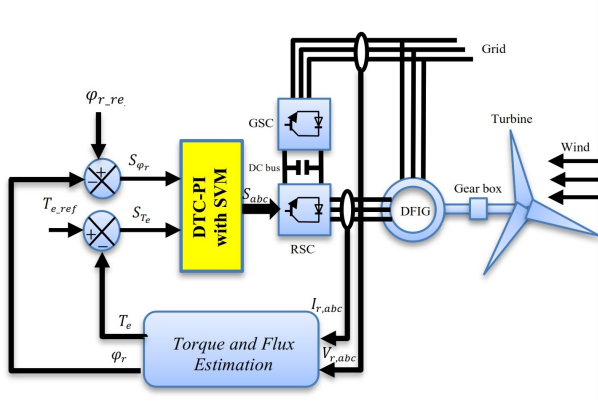


Fig. 3: Traditional DTC technique for the DFIG.

a two-level SVM inverter is used to control the DFIG rotor. Due to its simplicity, the PWM technique can generate control signals in IGBTs, while reducing the cost of implementation and simplifying the system. However, the system is less robust compared to the SVM technique.

Eq. (9) represents how to calculate the direct and quadrature rotor flux of the DFIG

$$\begin{cases} \Psi_{qr} = \int_0^t (-R_r i_{qr} + V_{qr}) dt \\ \Psi_{dr} = \int_0^t (-R_r i_{dr} + V_{dr}) dt \end{cases} \quad (9)$$

The following equation can calculate the magnitude flux:

$$\Psi_r = \sqrt{\Psi_{qr}^2 + \Psi_{dr}^2} \quad (10)$$

Eq. (11) represents the phase of rotor flux of the DFIG. The phase can be calculated using both direct and quadrature rotor flux of the DFIG.

$$\theta_r = \arctg \left(\frac{\Psi_{qr}}{\Psi_{dr}} \right) \quad (11)$$

The stator flux is related to stator voltage, as represented by Eq. (12). With this equation, the stator flux and stator voltage can be calculated.

$$|\overline{\Psi_s}| = \frac{|\overline{V_s}|}{\omega_s} \quad (12)$$

To estimate the flux and torque, the rotor voltage, and current must be measured. The rotor current and stator flux are required due to their relationship with the torque. On the other hand, the torque is also related to the resistance value. Eq. (13) represents the torque estimation used in this work.

$$T_e = \frac{3}{2} \frac{M}{L_s} n_p (-\Psi_{ds} I_{qr} + \Psi_{qs} I_{dr}) \quad (13)$$

Eq. (14) represents the estimation of the stator flux.

$$\begin{cases} \Psi_{ds} = \int_0^t (-R_s i_{qs} + V_{qs}) dt \\ \Psi_{qs} = \int_0^t (-R_s i_{ds} + V_{ds}) dt \end{cases} \quad (14)$$

Eqs. (15) and (16) represent the phase and magnitude of the stator flux, respectively.

$$\theta_s = \arctg \left(\frac{\Psi_{s\beta}}{\Psi_{s\alpha}} \right) \quad (15)$$

$$\Psi_s = \sqrt{\Psi_{s\alpha}^2 + \Psi_{s\beta}^2} \quad (16)$$

The DTC-PI technique involves a simple algorithm and is easier to use and more robust than the vector control, FOC, and DTC techniques. It is widely accepted that a PI controller reduces the degree of durability and increases the rate of ripples, especially when changing the system parameters. Consequently, the current quality is low, which is undesirable. However, the problems with torque fluctuation and changing the machine parameters remain. In this case, this control loses its durability and gives more torque and flux ripples. To solve these problems, it is suggested that the proposed nonlinear controllers be used. These proposed nonlinear controllers are explained in Section 4.

4. PROPOSED NONLINEAR CONTROLLERS

This section proposes and confirms the suitability of two different nonlinear controllers using the DTC strategy. The first is the FOSTA controller and the FOSOSMC. These nonlinear controllers are simpler, easy to implement, and more robust than the PI, STA, and SOCSMC. The two proposed nonlinear controllers are based on FO control to achieve robustness while improving the performance and characteristics of the traditional DTC strategy.

The FOC is a mathematical technique involving the generalization of integration and normal differentiation to arbitrary non-integer orders [38]. The use of this strategy gives very satisfactory results, as evidenced by previous work carried out in this field. It is not limited to mathematics alone but can also be applied to physics and electricity.

In this work, the FOC technique is used to improve the performance and effectiveness of both STA and SCOSMC controllers due to features such as its simplicity and durability.

The STA controller can be expressed by Eq. (17) [39].

$$u(t) = u_1(t) + u_2(t) \quad (17)$$

$u(t)$ is the output of the proposed STA controller. Where

$$u_1(t) = \lambda_1 \sqrt{|S|} \cdot \text{sign}(S) \quad (18)$$

$$u_2(t) = \lambda_2 \int \text{sign}(S) dt \quad (19)$$

The proposed FOSTA controller differs from the traditional STA in that simplicity is one of its biggest advantages. Eq. (20) expresses the controller proposed in this work, where α is the proposed FO control ($\alpha \neq 0$).

$$w(t) = \left(\lambda_1 \sqrt{|S|} \cdot \text{sign}(S) + \lambda_2 \int \text{sign}(S) \cdot dt \right)^\alpha \quad (20)$$

where $w(t)$ is the output of the FOSTA controller, and α is an adjustable parameter by which the performance and durability of the entire system can be greatly improved. If it is 1, the proposed FOSTA controller becomes a traditional STA controller. The proposed FOSTA controller is a simple algorithm, more robust, and easy to adjust. It also gives better results than the traditional STA controller [39]. Fig. 4 shows the proposed FOSTA controller.

The second suggested nonlinear controller is the FOSOCSCM, based on SOCSMC and fractional-order control theory. The proposed FOSOCSCM controller is more robust than the traditional SOCSMC, PI, and STA controllers. The SOCSMC principle can be illustrated by the following equation [32]:

$$y(t) = -K_1 |S|^{a_1} \text{sign}(s) - K_2 \cdot \text{sign}|S|^{1/2} + \int \alpha \cdot \text{sign}(s) dt \quad (21)$$

where S is the surface. K_1 and K_2 represent the constant gains.

The FOSOCSCM is a combination of fractional order control and the SOCSMC controller. The FOC technique is introduced into the SOCSMC controller to increase durability and maintain the simplicity of the SOCSMC. In similarity to the FOSTA controller, the proposed FOSOCSCM can be expressed by Eq. (22), where the λ is the proposed fractional order control used in this work ($\lambda \neq 0$).

$$Y(t) = (-K_1 |S|^{a_1} \text{sign}(S) - K_2 \cdot \text{sign}|S|^{1/2} + \int \alpha \cdot \text{sign}(S) dt)^\lambda \quad (22)$$

where K_1 and K_2 represent the constant gains.

$Y(t)$ is the output of the proposed FOSOCSCM controller.

Eq. (22) represents the proposed FOSOCSCM controller. K_1 and K_2 control the stability of the FOSOCSCM. On the other hand, λ represents the FO control and $\lambda \neq 0$. It can take positive or negative values, depending on the system used. If λ is equal to 1, the proposed controller becomes the classical controller. Fig. 5 shows the proposed FOSOCSCM controller used in this work which gives better results than the traditional SOCSMC controller.

The proposed FOSTA and FOSOCSCM controllers are used to improve the performance and effectiveness of the traditional DTC technique, while also reducing the THD value of the stator current and torque ripples. The

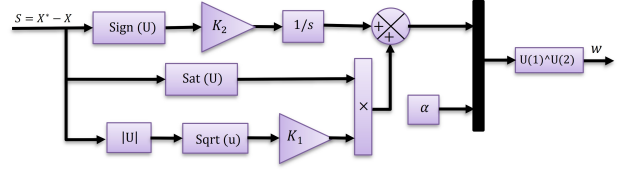


Fig. 4: Proposed FOSTA controller.

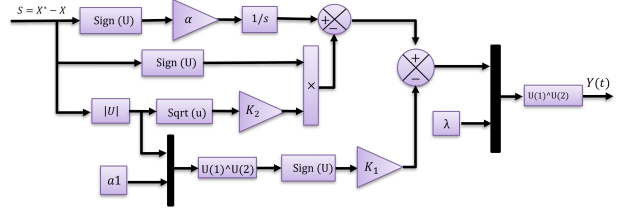


Fig. 5: Proposed FOSOCSCM controller.

proposed nonlinear DTC techniques in this paper are detailed in Section 5.

5. PROPOSED NONLINEAR DTC TECHNIQUES

This section proposes two different approaches to the nonlinear DTC control of the DFIG-based wind turbine. The first control is the DTC-FOSTA technique, and the second the DTC-FOSOCSCM. Durability, simplicity, and ease of implementation are the main elements characterizing each proposed control. Moreover, the two proposed control schemes give very satisfactory results compared to the classical DTC strategy.

5.1 Design of the Proposed DTC-FOSTA Strategy

The proposed DTC-FOSTA represents a modification of the traditional DTC strategy. The proposed FOSTA controller replaces the hysteresis comparator to provide a more robust DTC strategy, while the two-level SVM technique replaces the switching table. Fig. 6 presents the proposed DTC-FOSTA technique. Compared to the traditional DTC technique, this control scheme is simple, easy to implement, robust, and has a fast response dynamic. In contrast to the classical DTC strategy, the proposed DTC-FOSTA technique reduces torque and flux ripples. Fig. 7 shows the internal structure of the proposed DTC-FOSTA technique. The proposed DTC-FOSTA uses the same torque and flux estimation equations as the classical DTC technique explained in Section 3 of this paper.

The torque and rotor flux FOSTA controllers influence the two rotor voltage components, as in Eqs. (23) and

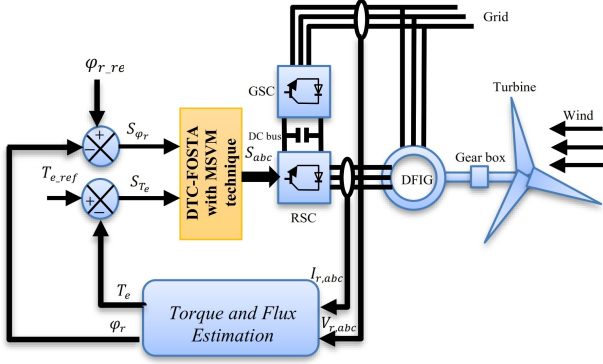


Fig. 6: The DTC-FOSTA technique of DFIG.

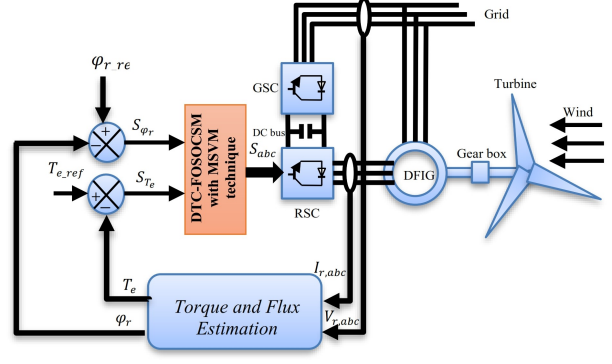


Fig. 10: The DTC-FOSOCMSM strategy of the DFIG.

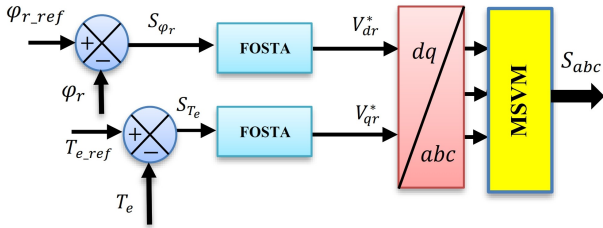


Fig. 7: Internal structure of the DTC-FOSTA technique.

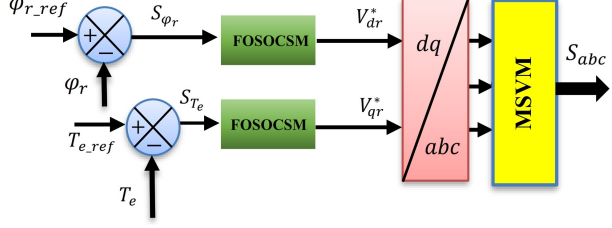


Fig. 11: Internal structure of the DTC-FOSOCMSM strategy.

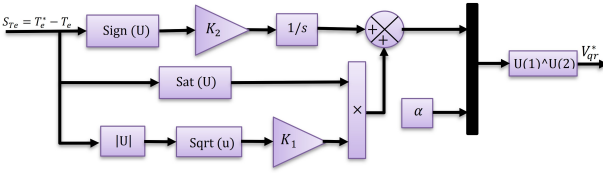


Fig. 8: Proposed FOSTA torque controller.

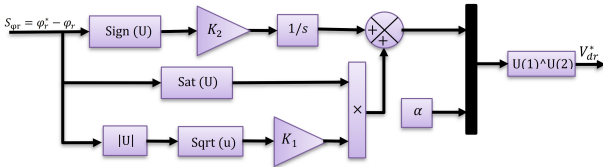


Fig. 9: Proposed FOSTA rotor flux controller.

(24).

$$V_{dr}^* = \left(\lambda_1 \sqrt{|S_{\varphi_r}|} \cdot \text{sign}(S_{\varphi_r}) + \lambda_2 \int \text{sign}(S_{\varphi_r}) \cdot dt \right)^\alpha \quad (23)$$

$$V_{qr}^* = \left(\lambda_1 \sqrt{|S_{T_e}|} \cdot \text{sign}(S_{T_e}) + \lambda_2 \int \text{sign}(S_{T_e}) \cdot dt \right)^\alpha \quad (24)$$

where S_{φ_r} is the rotor flux surface ($S_{\varphi_r} = \varphi_r^* - \varphi_r$), S_{T_e} is the torque surface ($S_{T_e} = T_e^* - T_e$).

Figs. 8 and 9 show the proposed FOSTA torque and FOSTA rotor flux controllers. As can be observed, the new proposed nonlinear controller is very simple and can be easily accomplished.

5.2 Design of the Proposed DTC-FOSOCMSM Technique

Using the same implementation method as the DTC-FOSTA, the traditional hysteresis comparator is replaced by the proposed FOSOCMSM controller designed in Section 3. The objective of the proposed DTC-FOSOCMSM technique is to control the torque and flux as well as reduce ripples and the THD value of stator current. Robustness is one of the biggest advantages of the proposed DTC-FOSOCMSM strategy. It involves a simple algorithm and can be easily implemented. A block diagram of the proposed DTC-FOSOCMSM strategy is shown in Fig. 10, while Fig. 11 presents a block diagram of the DTC-FOSOCMSM strategy.

The torque and rotor flux FOSOCMSM controllers influence the two rotor voltage components, as in Eqs. (25) and (26).

$$V_{dr}^* = (-K_1 |S_{\varphi_r}|^{a_1} \text{sign}(S_{\varphi_r}) - K_2 \cdot \text{sign}|S_{\varphi_r}|^{1/2} + \int \alpha \cdot \text{sign}(S_{\varphi_r}) dt)^\lambda \quad (25)$$

$$V_{qr}^* = (-K_1 |S_{T_e}|^{a_1} \text{sign}(S_{T_e}) - K_2 \cdot \text{sign}|S_{T_e}|^{1/2} + \int \alpha \cdot \text{sign}(S_{T_e}) dt)^\lambda \quad (26)$$

The proposed rotor flux and torque FOSOCMSM controllers are shown in Figs. 12 and 13, respectively.

6. RESULTS

In this section, three DTC techniques are proposed, simulated, and compared to identify which of them is

Table 3: Comparison between the results obtained from the proposed nonlinear DTC techniques and the DTC-PI control.

| Criteria | Control Methods | | |
|-------------------------------------------|-----------------|--------------------|--------------------|
| | DTC-PI | DTC-FOSOCSCMC | DTC-FOSTA |
| Flux and torque tracking | Acceptable | Good | Excellent |
| THD (%) | 0.74 | 0.33 | 0.17 |
| Dynamic response (s) | Medium | Fast | Fast |
| Settling time (ms) | High | Medium | Medium |
| Reduce torque and flux ripples | Acceptable | Very good | Excellent |
| Overshoot (%) | 21% | 1.2% | 1% |
| Simplicity of converter and filter design | Simple | Simple | Simple |
| Current ripple (A) | Around 30 | Around 10 | Around 4 |
| Torque ripple (Nm) | Around 400 | Around 100 | Around 50 |
| Rise time (s) | High | Medium | Medium |
| Simplicity of calculations | Simple | Rather complicated | Rather complicated |
| Flux ripple (wb) | Around 0.02 | Around 0.003 | Around 0.001 |
| Improvement of transient performance | Good | Excellent | Excellent |
| Quality of stator current | Acceptable | Very good | Excellent |

Table 4: Comparison of the effect ratio between the designed and traditional techniques.

| Strategy | THD (%) | Ratio (%) |
|---------------|---------|-----------|
| DTC-FOSTA | 0.23 | 54.90 |
| DTC-FOSOCSCMC | 0.12 | 76.47 |

Table 5: Results of the first test.

| Criteria | in DTC | Strategy 1 | Strategy 2 |
|----------------------|------------|------------|------------|
| THD (%) | 0.51 | 0.23 | 0.12 |
| Rise time (s) | High | Medium | Medium |
| Flux ripples (wh) | 0.01 | 0.0064 | 0.0021 |
| Torque ripples (Nm) | 980 | 200 | 60 |
| Quality of current | Low | Medium | High |
| Overshoot (%) | ≈ 30% | ≈ 2% | ≈ 1.5% |
| Settling time (ms) | High | Medium | Medium |
| Tracking references | Acceptable | Good | Very good |
| Dynamic response (s) | Medium | Fast | Fast |
| Steady-state error | High | Medium | Low |
| Current ripples (A) | 40 | 28 | 17 |

Note: Strategy 1 is the DTC-FOSOCSCMC and strategy 2 the DTC-FOSTA technique

Table 6: Results of the second test.

| Criteria | in DTC | Strategy 1 | Strategy 2 |
|----------------------|------------|------------|------------|
| THD (%) | 0.51 | 0.23 | 0.12 |
| Rise time (s) | High | Medium | Medium |
| Flux ripples (wh) | 0.014 | 0.0041 | 0.0038 |
| Torque ripples (Nm) | 770 | 52 | 31 |
| Quality of current | Low | Medium | High |
| Overshoot (%) | ≈ 19% | ≈ 1.5% | ≈ 1% |
| Settling time (ms) | High | Medium | Medium |
| Tracking references | Acceptable | Good | Very good |
| Dynamic response (s) | Medium | Fast | Fast |
| Steady-state error | High | Medium | Low |
| Current ripples (A) | 27 | 17 | 8 |

Note: Strategy 1 is the DTC-FOSOCSCMC and strategy 2 the DTC-FOSTA technique

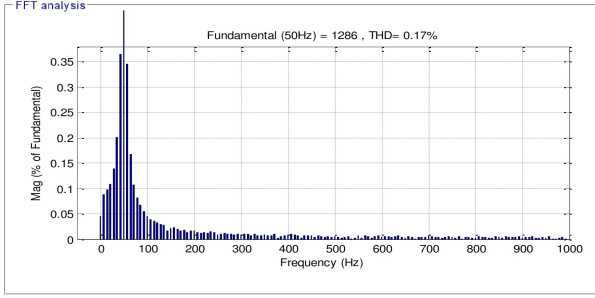


Fig. 19: THD (DTC-FOSTA).

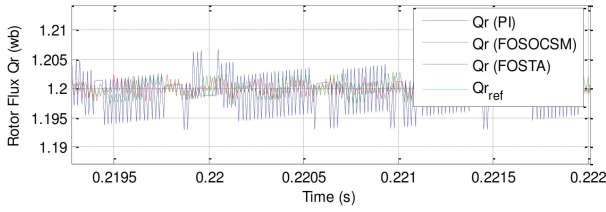


Fig. 20: Zoom of the flux.

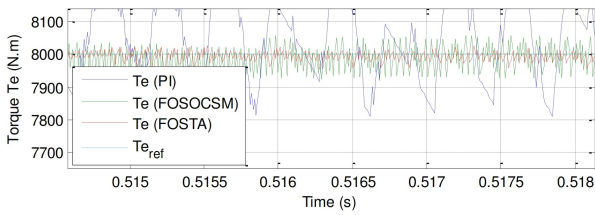


Fig. 21: Zoom of the torque.

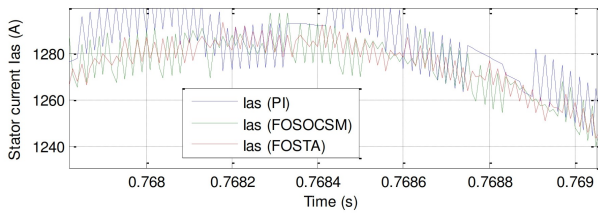


Fig. 22: Zoom of the current.

6.2 Robustness Test

The principal objective of the robustness test is to examine the influence of variations in DFIG parameters on the current, rotor flux, THD value, torque, and behavior of three proposed DTC strategies. The obtained results presented in Figs. 23 to 31 indicate that the torque and rotor flux follow the references well for all the proposed controls (see Figs. 23 and 24). As for the stator current, its value remains related to the system and reference value of the torque (see Fig. 25).

Changing the DFIG parameters led to a change in the THD value for all three DTC techniques. However, the DTC-FOSTA technique still gives less value than other controls. Table 4 presents the percentage reduction of THD for the classical control, indicating that the DTC-FOSTA technique provides much larger percentages than

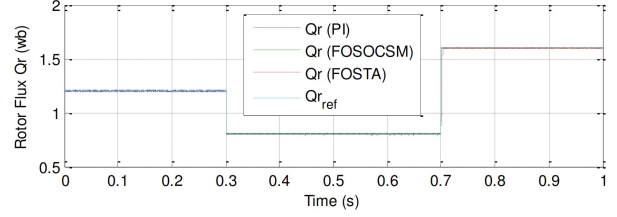


Fig. 23: Rotor flux.

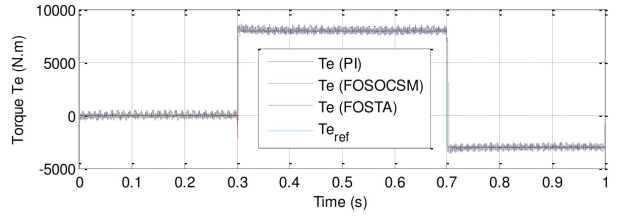


Fig. 24: Torque.

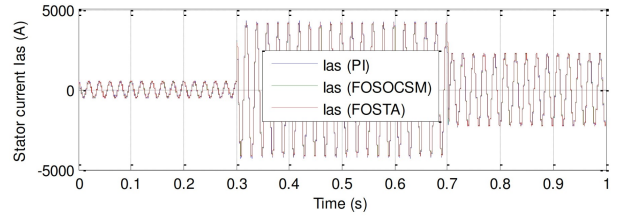


Fig. 25: Current.

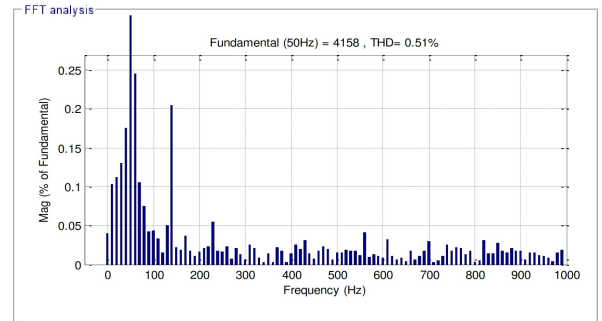


Fig. 26: THD (DTC-PI).

the DTC-FOSOCSCM strategy. As for the percentage reduction compared to the DTC-FOSOCSCM strategy, it is about 47.82%. These percentages are very acceptable and indicate the robustness of this technique (DTC-FOSTA) compared to the remainder of the proposed DTC techniques.

The results of the DTC-FOSOCSCM and DTC-PI control strategies are presented in Table 5. As can be observed, the DTC-FOSTA technique is better than the other control schemes in all respects. The DTC-FOSTA technique reduced the torque ripple value by about 93.87% compared to the classical DTC strategy. The DTC-FOSOCSCM reduced the torque ripple by an estimated 79.59% compared to the classical DTC technique. It can therefore be concluded that the DTC-

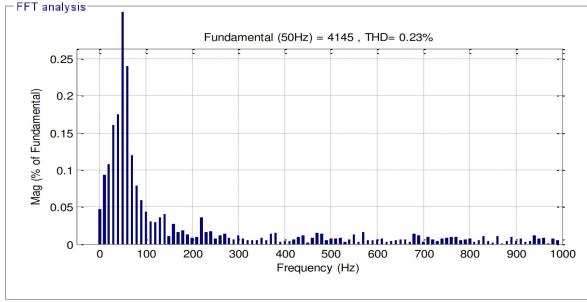


Fig. 27: THD (DTC-FOSOCSCM).

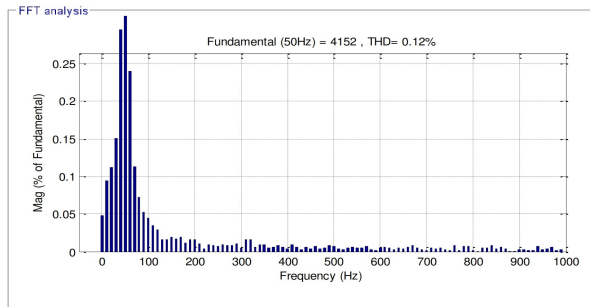


Fig. 28: THD (DTC-FOSTA).

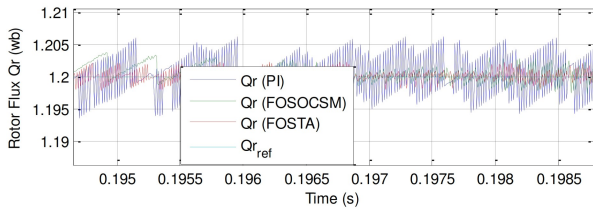


Fig. 29: Zoom of the flux.

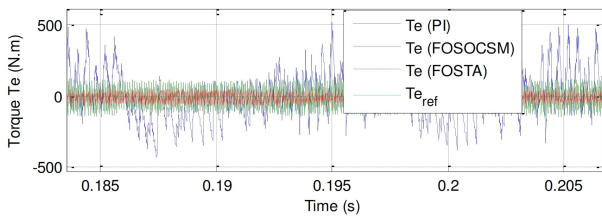


Fig. 30: Zoom of the torque.

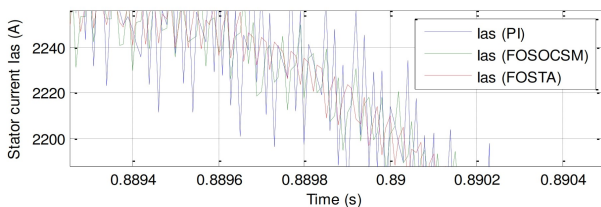


Fig. 31: Zoom of the current.

FOSTA technique is better than the DTC-FOSOCSCM in reducing torque ripples. The same applies to the stator current ripples, where the percentage reduction

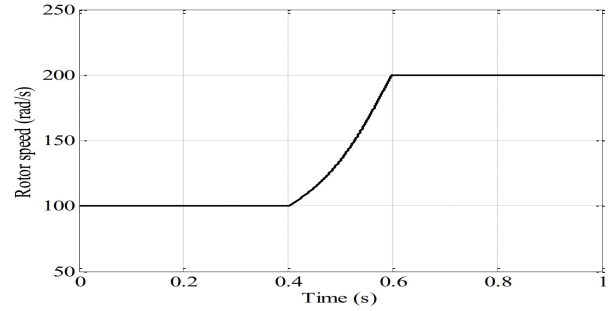


Fig. 32: Rotor speed profile.

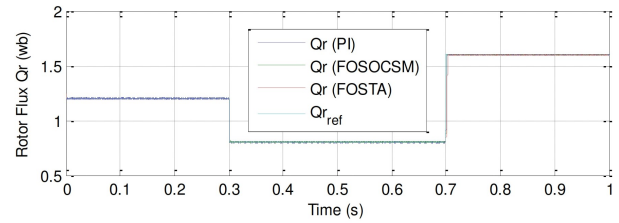


Fig. 33: Rotor flux.

percentage was about 30% for the DTC-FOSOCSCM and 57.50% for the DTC-FOSTA techniques compared to the classical DTC strategy. Furthermore, the rotor flux reduction ratios compared to the traditional DTC technique were approximately 36% and 79% for the DTC-FOSOCSCM and DTC-FOSTA techniques, respectively.

6.3 Sensibility Test

In the sensibility test, the rotor speed is varied at different time intervals. Fig. 32 shows the rotor speed of the DFIG. The principal objective of this test is to examine the influence of a mechanical speed variation in the DFIG on the rotor flux and torque behaviors of the three proposed DTC techniques. The obtained results are presented in Figs. 33 to 41. Figs. 33 to 35 show that the torque and flux follow the references well, with the DTC-FOSTA being the preferred technique in terms of dynamic response compared to the remaining techniques. It can also be observed that the flux and torque change are not related to the three proposed techniques, confirming their robustness. Most of the results obtained from this test are presented in Table 6. The electric current of the three modes is shown in Fig. 35. As can be observed, the electric current is sinusoidal with a frequency of 50 Hz, whereby the current changes are unrelated to the rotor speed profile of the three modes. The electric current takes the same form as the torque, with its value related to that of the torque. Therefore, an increase in the value of the torque leads to an increase in the value of the resulting current and vice versa.

The ripples of torque, flux, and current are presented in Figs. 36, 37, 38, and Table 6. As can be observed, the DTC-FOSTA technique significantly reduced these ripples compared to the classical DTC technique, as

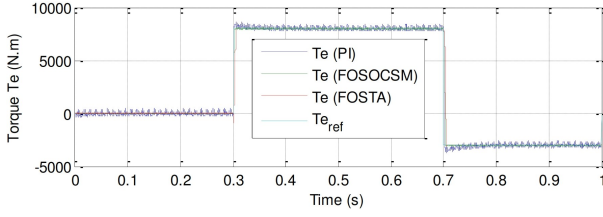


Fig. 34: Torque.

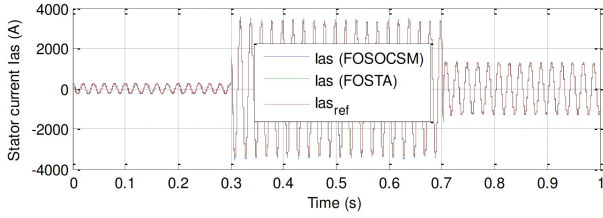


Fig. 35: Current.

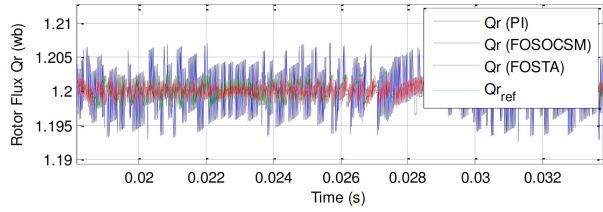


Fig. 36: Zoom of the flux.

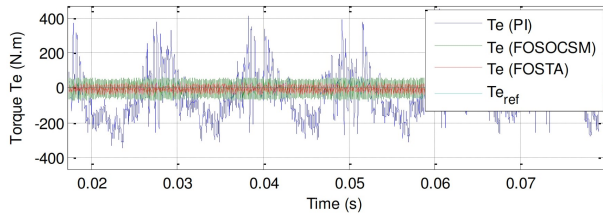


Fig. 37: Zoom of the torque.

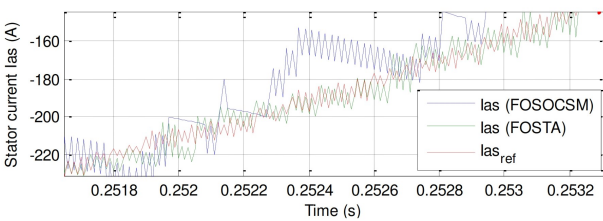


Fig. 38: Zoom of the current.

indicated by the obtained ripple values. Whereas the speed variation produces a negligible effect on the rotor flux, current, THD value, torque, and curves for both DTC techniques. Furthermore, the DTC-FOSTA technique reduced the ripples of torque, current, and flux by about 93.24%, 37.03%, and 70.71%, respectively, compared to the classical DTC technique. Compared with the DTC-FOSOCSCM technique, the DTC-FOSTA technique reduced the current, torque, and flux ripples by about

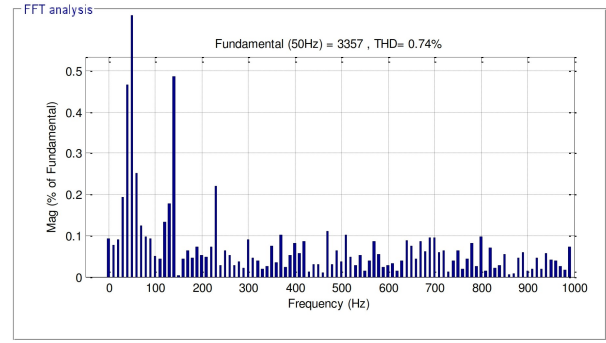


Fig. 39: THD (DTC-PI).

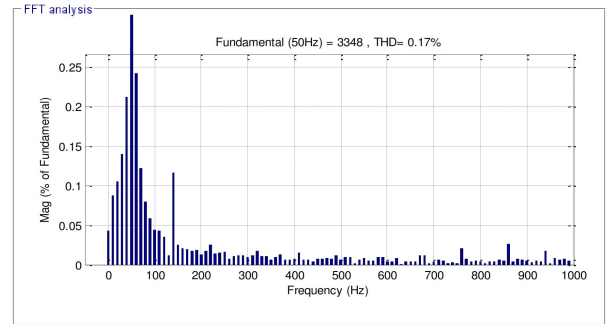


Fig. 40: THD (DTC-FOSOCSCM).

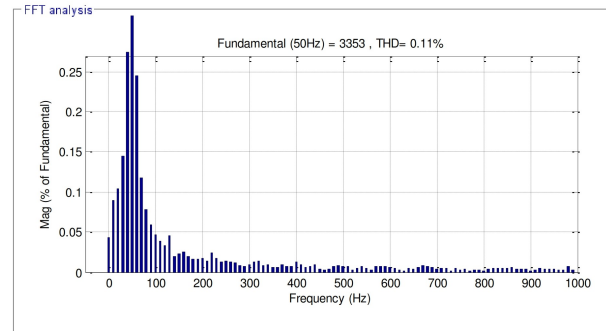


Fig. 41: THD (DTC-FOSTA).

52.94%, 40.38%, and 7.31%, respectively. Accordingly, it can be said that the DTC-FOSTA technique is the best solution for controlling electrical power generation.

Figs. 39, 40, and 41 show the THD value of the current for the designed DTC techniques. It should be noted that the THD value is lower for DTC-FOSTA (0.11%) compared to DTC (0.74%) and DTC-FOSOCSCM (0.17%). These results indicate that the DTC-FOSTA technique reduces the THD value by 85.13% and 35.29% compared with the DTC and DTC-FOSOCSCM, respectively.

Finally, the THD value of the current is compared between the proposed nonlinear DTC techniques and several published works, the results of which are presented in Table 7. As can be observed, the proposed nonlinear DTC strategies gave much lower THD values than some published strategies, such as FOC, fuzzy DTC,

Table 7: Summary of comparative results.

| Reference | Techniques | THD (%) |
|---------------------|----------------------------------------------------|---------|
| [27] | DTC control | 6.70 |
| | Fuzzy DTC control | 2.04 |
| [32] | DTC-SOCSMC | 0.95 |
| [40] | 12 sectors DPC control | 0.40 |
| [41] | DPC with IP controllers | 0.43 |
| [42] | DARPC control with STA controller | 1.66 |
| [2] | DPC with terminal synergetic controller | 0.25 |
| [43] | SOSMC method | 3.13 |
| [44] | FOC with neuro-fuzzy controller (FOC-NFC) | 0.78 |
| | FOC with Type 2 fuzzy logic controller (FOC-T2FLC) | 1.14 |
| [45] | Integral SMC technique | 9.71 |
| | Multi-resonant-based sliding mode controller | 3.14 |
| [46] | Fuzzy SMC method | 1.15 |
| [47] | Direct FOC control | 2.94 |
| | Direct FOC with third-order sliding mode | 1.42 |
| [3] | Direct FOC control | 1.45 |
| | Direct FOC with synergetic-sliding mode | 0.50 |
| Proposed strategies | DTC-FOSOCSCM | 0.17 |
| | DTC-FOSTA | 0.11 |

and DPC. It can therefore be concluded that the proposed DTC-FOSTA strategy gives a sinusoidal current which gives an effective performance in terms of current, flux, and torque ripples. It also has a better THD value than the remainder of the published works, thereby increasing device longevity and reducing maintenance costs.

7. CONCLUSION

In this study, three DTC techniques are proposed for controlling the DFIG-based wind turbine, with the strengths of each compared to the remaining published works. Furthermore, the new nonlinear techniques have been embodied using MATLAB/Simulink software. The values of the designed nonlinear DTC techniques were compared in terms of torque and flux ripples, trace references, and the extent of influence in the case of changes in machine parameters.

The numerical simulation results evidence the efficiency of the adopted technique (DTC-FOSTA), especially in attenuating the ripples at the flux and torque levels due to the elimination of PI controllers and improvement in screw robustness. Furthermore, the DTC-FOSTA technique addresses the parametric variation issue and alleviates the chattering phenomenon.

The DTC-FOSTA technique provides an improvement over the DTC and DTC-FOSOCSCM techniques. This improvement is remarkable, especially in terms of the torque ripple, current quality, rotor flux ripple, value

of THD, and the dynamic responses of torque and rotor flux. THD minimization can be estimated at 85% and 35% compared to the DTC and DTC-FOSOCSCM techniques, making it possible to limit the ripples at different electrical quantities. The minimization ratios were about 95%, 86%, and 87% for rotor flux, current, and torque, respectively, compared to the DTC technique. On the other hand, DTC-FOSTA reduced the values of ripples in current (60%), torque (50%), and flux (66%) compared to the DTC-FOSOCSCM strategy.

Although these percentages are high and indicate the robustness of the designed DTC-FOSTA technique for improving the performance of the DFIG-based wind turbine, the ripples, torque, and flux problems cannot be eliminated entirely. Therefore, for a more satisfactory improvement, futurework should take advantage of a technique based on artificial intelligence to further improve the performance of the DTC-DFIG system.

The current injected into the grid has a low THD value of 0.11%. The proposed nonlinear DTC-FOSTA strategy presents less rotor flux, torque, and current ripples than the DFIG-based wind turbine system.

In summary, the main findings of this research are as follows:

- A new FO high-order SMC technique, confirmed with numerical simulation.
- A new DTC strategy based on FO high-order SMC techniques for comparison with the traditional DTC technique.
- A reduction in the harmonic distortion value of the current.
- Minimization of the torque, current, and rotor flux ripples.
- A different robust nonlinear DTC technique, designed and confirmed using MATLAB software.

A future study will be conducted to improve the quality of torque and flux, with the DFIG controlled using other proposed nonlinear strategies such as the terminal-STA method, fuzzy third-order SMC technique, and fast terminal synergetic control.

NOMENCLATURE

| | |
|----------|------------------------------------------------------------------|
| DFIG | Doubly-fed induction generator |
| DTC | Direct torque control |
| PI | Proportional-Integral |
| SVM | Space vector modulation |
| PWM | Pulse width modulation |
| STA | Super twisting algorithm |
| SOCSMC | Second-order continuous sliding mode controller |
| SMC | Sliding mode controller |
| THD | Total harmonic distortion |
| FOSTA | Fractional-order super twisting algorithm |
| FOC | Field-oriented control |
| FOC | Fractional-order control |
| FOSOCSCM | Fractional-order second-order continuous sliding mode controller |
| T2FLC | Type 2 fuzzy logic controller |

| | |
|-----|------------------------|
| DPC | Direct power control |
| FLC | Fuzzy logic controller |
| NFC | Neuro-fuzzy controller |
| IP | Integral proportional |

REFERENCES

- [1] B. Lukutin, K.H. Kadhim, A.N. Jbarah and O. Karrar, "Energy systems modelling and simulation of behavior for AGBWT in isolated network using Simulink/MatLab," *Test Eng Manage*, vol. 83, no. 5-6, pp. 15245-15249, 2020.
- [2] H. Benbouhenni and N. Bizon, "A synergetic sliding mode controller applied to direct field-oriented control of induction generator-based variable speed dual-rotor wind turbines," *Energies*, vol. 14, no. 15, pp. 4437, Aug. 2021.
- [3] H. Benbouhenni and N. Bizon, "Terminal synergetic control for direct active and reactive powers in asynchronous generator-based dual-rotor wind power systems," *Electronics*, vol. 10, no. 16, pp. 1880, Aug. 2021.
- [4] H. Benbouhenni and Z. Boudjema, "Two-level DTC based on ANN controller of DFIG using 7-level hysteresis command to reduce flux ripple comparing with traditional command," In *2018 International Conference on Applied Smart Systems (ICASS)*, Medea, Algeria, 2018, pp. 1-8.
- [5] A. Ardjal, M. Bettayeb, R. Mansouri, and A. Mehiri, "Nonlinear synergetic control approach for Dc-Link voltage regulator of wind turbine DFIG connected to the grid," in *5th International Conference on Renewable Energy: Generation and Application (ICREGA)*, Al Ain, United Arab Emirates, 2018, pp. 94-97.
- [6] P. Xiong and D. Sun, "Backstepping-based DPC strategy of a wind turbine-driven DFIG under Normal and Harmonic Grid Voltage," *IEEE Transactions on Power Electronics*, vol. 31, no. 6, pp.4216-4225, Jun. 2016.
- [7] K. Qingmei, W. Xiangdong, and L. Shujiang, "A novel sliding mode control of doubly-fed induction generator for optimal power extraction," In *2019 IEEE Innovative Smart Grid Technologies-Asia (ISGT Asia)*, Chengdu, China, 2019, pp. 1318-1323.
- [8] H. Benbouhenni, Z. Boudjema, and A. Belaidi, "Power Control of DFIG in WECS Using DPC and NDPC-NPWM Methods," *Mathematical Modelling of Engineering Problems*, vol. 7, no. 2, pp. 223-236, Jun. 2020.
- [9] R. M. Prasad and M. A. Mulla, "Mathematical modeling and position-sensorless algorithm for stator-side field-oriented control of rotor-tied DFIG in rotor flux reference frame," *IEEE Transactions on Energy Conversion*, vol. 35, no. 2, pp.631-639, Jun. 2020.
- [10] M. A. Mossa, T. Duc Do, A. Saad Al-Sumaiti, N. V. Quynh, and A. A. Z. Diab, "Effective model predictive voltage control for a sensorless doubly fed induction generator," *IEEE Canadian Journal of Electrical and Computer Engineering*, vol. 44, no. 1, pp. 50-64, Jan. 2021.
- [11] H. Benbouhenni, "Comparison study between seven-level SVPWM and two-level SVPWM strategy in direct vector control of a DFIG-based wind energy conversion systems," *International Journal of Applied Power Engineering (IJAPE)*, vol. 9, no. 1, pp. 12-21, Apr. 2020.
- [12] X. Zhu, S. Liu, and Y. Wang, "Second-order sliding-mode control of DFIG-based wind turbines," in *3rd Renewable Power Generation Conference (RPG 2014)*, Naples, 2014, pp. 1-6.
- [13] L. Xiong, J. Wang, X. Mi, and M. W. Khan, "Fractional order sliding mode based direct power control of grid-connected DFIG," *IEEE Transactions on Power Systems*, vol. 33, no. 3, pp. 3087-3096, May 2018.
- [14] M. Sellah, A. Kouzou, M. Mohamed-Seghir, M. M. Rezaoui, R. Kennel, and M. Abdelrahman, "Improved DTC-SVM based on input-output feedback linearization technique applied on DOEWIM powered by two dual indirect matrix converters," *Energies*, vol. 14, no. 18, pp. 5625, Sep. 2021.
- [15] A. Nasr, C. Gu, S. Bozhko, and C. Gerada, "Performance enhancement of direct torque-controlled permanent magnet synchronous motor with a flexible switching table," *Energies*, vol. 13, no. 8, pp. 1907, Apr. 2020.
- [16] Y. Zhou, D. Zhang, X. Chen, and Q. Lin, "Sensorless direct torque control for saliency permanent magnet brushless DC motors," *IEEE Transactions on Energy Conversion*, vol. 31, no. 2, pp.446-454, Jun. 2016.
- [17] Z. Zhang, Y. Zhao, W. Qiao, and L. Qu, "A Discrete-time direct torque control for direct-drive PMSG-based wind energy conversion systems," *IEEE Transactions on Industry Applications*, vol. 51, no. 4, pp. 3504-3514, Jul.-Aug. 2015.
- [18] H. Benbouhenni, "Comparison study between SVPWM and FSVPWM strategy in fuzzy second order sliding mode control of a DFIG-based wind turbine," *Carpathian Journal of Electronic and Computer Engineering*, vol. 12, no. 2, pp. 1-10, Dec. 2019.
- [19] H. Heidari, A. Rassölkin, T. Vaimann, A. Kallaste, A. Taheri, M. H. Holakooie and A. Belahcen, "A novel vector control strategy for a six-phase induction motor with low torque ripples and harmonic currents," *Energies*, vol. 12, no. 6, pp.1102, Mar. 2019.
- [20] M. A. Mossa, H. Echeikh, A. a. Z. Diab, H. H. Alhelou, and P. Siano, "Comparative Study of Hysteresis Controller, Resonant Controller and Direct Torque Control of Five-Phase IM under Open-Phase Fault Operation," *Energies*, vol. 14, no. 5, pp. 1317, Feb. 2021.
- [21] Y. Zhou and G. Chen, "Predictive DTC strategy with fault-tolerant function for six-phase and three-

- phase PMSM series-connected drive system," *IEEE Transactions on Industrial Electronics*, vol. 65, no. 11, pp. 9101-9112, Nov. 2018.
- [22] H. Benbouhenni and N. Bizon, "Improved rotor flux and torque control based on the third-order sliding mode scheme applied to the asynchronous generator for the single-rotor wind turbine," *Mathematics*, vol. 9, no. 18, pp. 2297, Sep. 2021.
- [23] Y. Farajpour, M. Alzayed, H. Chaoui, and S. Kelouwani, "A novel switching table for a modified three-level inverter-fed DTC drive with torque and flux ripple minimization," *Energies*, vol. 13, no. 18, pp. 4646, Sep. 2020.
- [24] Z. Zhou, X. Gu, Z. Wang, G. Zhang, and Q. Geng, "An improved torque control strategy of PMSM drive considering on-line MTPA operation," *Energies*, vol. 12, no. 15, pp. 2951, Jul. 2019.
- [25] Q. Song, Y. Li, and C. Jia, "A novel direct torque control method based on asymmetric boundary layer sliding mode control for PMSM," *Energies*, vol. 11, no. 3, pp. 657, Mar. 2018.
- [26] G. Q. Bao, W. Qi, and T. He, "Direct torque control of PMSM with modified finite set model predictive control," *Energies*, vol. 13, no. 1, pp. 234, Jan. 2020.
- [27] W. Ayrir, M. Ourahou, B. el Hassouni, and A. Haddi, "Direct torque control improvement of a variable speed DFIG based on a fuzzy inference system," *Mathematics and Computers in Simulation*, vol. 167, pp. 308-324, Jan. 2020.
- [28] F. Mehedi, H. Benbouhenni, L. Nezli, and D. Boudana, "Feedforward neural network-DTC of multi-phase permanent magnet synchronous motor using five-phase neural space vector pulse width modulation strategy," *Journal European des Systemes Automatises*, vol. 54, no. 2, pp. 345-354, Apr. 2021.
- [29] F. Mehedi, A. Yahdou, A. B. Djilali, and H. Benbouhenni, "Direct torque fuzzy controlled drive for multi-phase IPMSM based on SVM technique," *Journal European des Systemes Automatises*, vol. 53, no. 2, pp. 259-266, May 2020.
- [30] H. Benbouhenni, "Utilization of an ANFIS-STSM algorithm to minimize total harmonic distortion," *International Journal of Smart grid*, vol. 4, no. 2, pp. 56-67, Jan. 2020.
- [31] H. Benbouhenni, "Torque ripple reduction of DTC DFIG drive using neural PI regulators," *Majlesi Journal of Energy Management*, vol. 8, no. 2, pp. 21-26, Jun. 2019.
- [32] Z. Boudjema, R. Taleb, Y. Djeriri, and A. Yahdou, "A novel direct torque control using second order continuous sliding mode of a doubly fed induction generator for a wind energy conversion system," *Turkish Journal of Electrical Engineering and Computer Sciences*, vol. 25, no. 2, pp. 965-975, Jan. 2017.
- [33] H. Benbouhenni and N. Bizon, "Advanced direct vector control method for optimizing the operation of a double-powered induction generator-based dual-rotor wind turbine system," *Mathematics*, vol. 9, no. 19, pp. 2403, Sep. 2021.
- [34] A. N. J. Almakki and A. A. Mazalov, "Application of fractional-order second-order continuous sliding mode controller in direct flux and torque control system of doubly-fed induction generator integrated to wind turbine: simulation studies," *Vestnik Gosudarstvennogo universiteta morskogo i rechnogo flota imeni admirala S. O. Makarova*, vol. 13, no. 6, pp. 887-907, Dec. 2021.
- [35] A. N. J. Almakki and A. A. Mazalov, "Improving the efficiency of direct flux and torque control technology for doubly-fed induction generator with a robust control using modified super-twisting algorithms," *Vestnik Gosudarstvennogo universiteta morskogo i rechnogo flota imeni admirala S. O. Makarova*, vol. 13, no. 4, pp. 586-603, Aug. 2021.
- [36] H. Benbouhenni, "Direct vector control for doubly fed induction generator-based wind turbine system using five-level NSVM and two-level NSVM technique," *International Journal of Smart Grid*, vol. 3, no. 1, pp. 25-32, Jan. 2019.
- [37] A. Azimi, F. Bakhtiari-Nejad, and W. Zhu, "Fractional-order control with second-order sliding mode algorithm and disturbance estimation for vibration suppression of marine riser," *Journal of the Franklin Institute*, vol. 358, no. 13, pp. 6545-6565, Sep. 2021.
- [38] A. P. Shah and A. J. Mehta, "Direct power control of DFIG using super-twisting algorithm based on second-order sliding mode control," in *2016 14th International Workshop on Variable Structure Systems*, Nanjing, China, 2016, pp. 136-141.
- [39] A. N. J. Almakki and A. Mazalov, "Improved DFIG DFTC by using a fractional-order super twisting algorithms in wind power application," *Modern Transportation Systems and Technologies*, vol. 7, no. 3, pp. 131-149, Sep. 2021.
- [40] N. A. Yusoff, A. M. Razali, K. A. Karim, T. Sutikno, and A. Jidin, "A concept of virtual-flux direct power control of three-phase AC-DC converter," *International Journal of Power Electronics and Drive Systems*, vol. 8, no. 4, pp. 1776, Dec. 2017.
- [41] F. Amrane, B. Francois, and A. Chaiba, "Experimental investigation of efficient and simple wind-turbine based on DFIG-direct power control using LCL-filter for stand-alone mode," *ISA Transactions*, vol. 125, no. 11, Jul. 2021.
- [42] I. Yaichi, A. Semmah, P. Wira, and Y. Djeriri, "Super-twisting sliding mode control of a doubly-fed induction generator based on the SVM Strategy," *Periodica polytechnica Electrical engineering and computer science*, vol. 63, no. 3, pp. 178-190, Jan. 2019.
- [43] A. Yahdou, B. Hemici, and Z. Boudjema, "Second order sliding mode control of a dual-rotor wind turbine system by employing a matrix converter," *Journal of Electrical Engineering*, vol. 16, no. 3, pp.

1-11, Jan. 2016.

- [44] F. Amrane and A. Chaiba, "A novel direct power control for grid-connected doubly fed induction generator based on hybrid artificial intelligent control with space vector modulation," *Revue Roumaine des Sciences Techniques Serie Electrotechnique et Energetique*, vol. 61, no. 3, Jan. 2016.
- [45] Y. Quan, L. Hang, Y. He, and Y. Zhang, "Multi-resonant-based sliding mode control of DFIG-based wind system under unbalanced and harmonic network conditions," *Applied Sciences*, vol. 9, no. 6, pp. 1124, Mar. 2019.
- [46] Z. Boudjema, A. Meroufel, Y. Djerriri and E. Bounadja, "Fuzzy sliding mode control of a doubly fed induction generator for wind energy conversion," *Carpathian Journal of Electronic and Computer Engineering*, vol. 6, no. 2, pp. 7, 2013.
- [47] H. Benbouhenni and N. Bizon, "Third-order sliding mode applied to the direct field-oriented control of the asynchronous generator for variable-speed contra-rotating wind turbine generation systems," *Energies*, vol. 14, no. 18, pp. 5877, Sep. 2021.



Ali Nadhim Jbarah Almakki received a B.S. degree in power and electrical machines from the University of Diyala, College of Engineering, Iraq, in 2006; the M.S. degree in electrical engineering from Kazan National Research Technical University named after A. N. Tupolev - KAI, Russia, in 2014, and the Ph.D. degree from Kazan National Research Technical University named after A. N. Tupolev - KAI, Russia, in 2022, where he is currently a Lecturer at the college of

engineering, University of Diyala, Iraq. His research interests include wind power systems, power electronics, electrical machines, and control.



Andrey A. Mazalov received a PhD degree in electrical power and machines from South Federal University in Russia (SFU) in 2013. Area of research interest: power systems simulation, renewable energy technologies, power system stability, Smart Grid and NILM technologies. He has 17 scientific research published in local and international journals. Area editor in EAI Endorsed Transactions on Energy Web journal.



H. Benbouhenni was born in Chlef, Algeria. He is a PhD in the Department of Electrical Engineering at the ENPO-MA, Oran, Algeria. He received a M.A. degree in Automatic and informatique industrial in 2017. He is currently a professor at the University of Nisantasi, Turkey. He is editor of seven books and more than 130 papers in scientific fields related to electrical engineering. His research activities include the application of robust control in wind turbine power systems.



Nicu Bizon (Senior Member, IEEE) was born in Albesti de Muscel, Arges county, Romania, 1961. He received the 5 years B.S. degree in electronic engineering from the University "Polytechnic" of Bucharest, Romania, in 1986, and a Ph.D. degree in Automatic Systems and Control from the same university, in 1996. From 1996 to 1989, he was in hardware design with the Dacia Renault SA, Romania. Since 2000, he is professor with the University of Pitesti, Romania. He received two awards

from Romanian Academy (in 2013 and 2016) and is doctor honoris causa of the Petroleum-Gas University of Ploiești (2018). He is editor and authorship of 8 books published in Springer and the author of 165 scientific papers published in WoS (citations = 1,546 and h-index = 26), respectively, 249 scientific papers published in Scopus (citations = 2,337 and h-index = 30). His current research interests include power electronic converters, fuel cell and electric vehicles, renewable energy, energy storage system, microgrids, and control and optimization of these systems.